Evolution of GOUNDRY, a cryptic subgroup of Anopheles gambiae s.l., and its impact on susceptibility to Plasmodium infection.

Jacob E. Crawford, Michelle M. Riehle, Kyriacos Markianos, Emmanuel Bischoff, Wamdaogo M. Guelbeogo, Awa Gneme, N'Fale Sagnon, Kenneth D Vernick, Rasmus Nielsen, Brian P. Lazzaro

Received Date : 06-May-2015
Revised Date : 02-Jan-2016
Accepted Date : 18-Jan-2016
Article type : Original Article

Title: Evolution of GOUNDRY, a cryptic subgroup of *Anopheles gambiae s.l.*, and its impact on susceptibility to *Plasmodium* infection.

Running Head: Evolution of the *Anopheles* GOUNDRY subgroup.

Authors: Jacob E. Crawford[1,2], Michelle M. Riehle[3], Kyriacos Markianos[4], Emmanuel Bischoff[5], Wamdaogo M. Guelbeogo[6], Awa Gneme[6], N'Fale Sagnon[6], Kenneth D. Vernick[5], Rasmus Nielsen[2]*, Brian P. Lazzaro[1]*.
* These authors contributed equally to this work.

Affiliations:
1. Department of Entomology, Cornell University, Ithaca, NY, USA
2. Department of Integrative Biology, University of California, Berkeley, Berkeley, CA, USA
3. Department of Microbiology, University of Minnesota, St. Paul, MN, USA
4. Program in Genomics, Children's Hospital Boston, Harvard Medical School
5. Unit for Genetics and Genomics of Insect Vectors, Institut Pasteur, Paris, France
6. Centre National de Recherche et de Formation sur le Paludisme, 1487 Avenue de l'Oubritenga, 01 BP 2208 Ouagadougou, Burkina Faso.

Corresponding Author: Jacob Crawford, Department of Integrative Biology, University of California, Berkeley, Berkeley, CA, USA, j.crawford@berkeley.edu

Key Words: *Anopheles gambiae*, malaria, population genetics, inbreeding, demography, speciation

Abstract:

The recent discovery of a previously unknown genetic subgroup of *Anopheles gambiae sensu lato* underscores our incomplete understanding of complexities of vector population demographics in *Anopheles*. This subgroup, named GOUNDRY, does not rest indoors as adults and is highly susceptible to *Plasmodium* infection in the laboratory. Initial description of GOUNDRY suggested it differed from other known *Anopheles* taxa in surprising and sometimes contradictory ways, raising a number of questions about its age, population size, and relationship to known subgroups. To address these questions, we sequenced the complete genomes of 12 wild-caught GOUNDRY specimens and compared these genomes to a panel of *Anopheles* genomes. We show that GOUNDRY is most closely related to *Anopheles coluzzii*, and the timing of cladogenesis is not recent, substantially predating the advent of agriculture. We find a large region of the X chromosome that has swept to fixation in GOUNDRY within the last 100 years, which may be an inversion that serves as a partial barrier to contemporary gene flow. Interestingly, we show that GOUNDRY has a history of inbreeding that is significantly associated with susceptibility to *Plasmodium* infection in the laboratory. Our results illuminate the genomic evolution of one of probably several cryptic, ecologically specialized subgroups of *Anopheles* and provide a potent example of how vector population dynamics may complicate efforts to control or eradicate malaria.

Introduction:

The continued devastating burden of malaria on human populations in sub-Saharan Africa (Murray *et al.* 2012; WHO 2013) spurs ongoing searches for novel means of controlling vector mosquitoes, including through genetic manipulation. However, it is becoming increasingly appreciated that *Anopheles* species frequently form partially

reproductively isolated and ecologically differentiated subpopulations (Costantini *et al.* 2009; Gnémé *et al.* 2013; Lee *et al.* 2013; Fontaine *et al.* 2015), which could complicate control efforts and extend disease transmission across seasons and micro-environmental space. As an example, a recent study showed that subgroups of *Anopheles gambiae sensu lato* have evolved distinct approaches for surviving the dry season resulting in the presence of vector populations throughout an extended proportion of the year (Dao *et al.* 2014). Comprehensive genomic analysis of evolutionary origins, demography, and adaptation will advance our understanding of such phenotypic divergence and its role in the formation of new *Anopheles* subgroups. Furthermore, genomic analysis of population diversity and genetic affinity among taxa can elucidate epidemiologically relevant aspects of population ecology like breeding structure and ecological distribution that are important for malaria control efforts.

Population structure analysis of a comprehensive *Anopheles* mosquito sampling effort along a 400-km transect in the Sudan-Savanna ecological zone of central Burkina Faso surprisingly revealed a previously unknown genetic cluster of *Anopheles gambiae sensu lato* (Riehle *et al.* 2011). The new subgroup, named GOUNDRY, was found in collections from larval pools but never in collections taken from inside human dwellings, implying an exophilic adult resting habit. GOUNDRY mosquitoes are highly susceptible to *Plasmodium* infection in the laboratory, but the feeding behavior of GOUNDRY adults is unknown. Thus it is unclear whether the subgroup is a major vector of human malaria.

Current knowledge of GOUNDRY is incomplete, with previous genetic understanding based on sparse microsatellite and SNP data (Riehle *et al.* 2011), but it is essential to global public health to understand the evolution of new subgroups such as GOUNDRY and how they may impact malaria control. GOUNDRY bears an atypical genetic profile for *Anopheles* in the Sudan-Savanna zone of West Africa that raises questions about its origins, such as whether it is a hybrid between *A. coluzzii* and *A. gambiae*, as well as how old it is, and how reproductively isolated it is from other *Anopheles* species. For example, the diagnostic SNPs that underlie one standard approach for distinguishing between *A. coluzzii* (previously *A. gambiae* M form) and *A. gambiae* (previously *A. gambiae* S form) were found to be segregating freely at Hardy-Weinberg Equilibrium (HWE) in GOUNDRY mosquitoes (Riehle *et al.* 2011), implying

that the population is either hybrid or that it predates the *gambiae-coluzzii* species split. Although high frequencies of hybrids diagnosed with these markers have been identified in coastal regions of West Africa (Ndiath *et al.* 2008; Oliveira *et al.* 2008; Caputo *et al.* 2011), hybrid genotypes are quite rare (<1%) in the region where GOUNDRY was collected (della Torre *et al.* 2001). An independent study used a slightly larger panel of SNPs that differentiate *A. coluzzii* and *A. gambiae* in the pericentromeric regions of the X chromosome and autosomes and found that typically diagnostic haplotypes were segregating at HWE in GOUNDRY with evidence of recombination among them (Lee *et al.* 2013). GOUNDRY also differed from typical *Anopheles s.l.* populations in the region in karyotype frequencies of the large 2L*a* chromosomal inversion. In the Sudan-Savanna zone, the inverted allele of the 2L*a* chromosomal inversion segregates near fixation in *A. coluzzii* and *A. gambiae* (Coluzzi *et al.* 1979), but both forms of the inversion are segregating at HWE frequencies in GOUNDRY (Riehle *et al.* 2011). Moreover, analysis of microsatellites and SNP markers revealed considerable distinction between GOUNDRY and other described *Anopheles* in the region and concluded that GOUNDRY is a genetic outgroup to *A. gambiae* and *A. coluzzii* (Riehle *et al.* 2011). However, GOUNDRY was less genetically variable than these other species, raising the possibility that, among other potential explanations, its origin may be more recent.

To identify the evolutionary origins, age, and degree of genetic isolation from other genetic subgroups of GOUNDRY, we analyzed full genome data from GOUNDRY and multiple closely related *Anopheles* species as well as SNP chip and phenotype data from an independent study (Mitri *et al.* 2015). We estimate the demographic history of GOUNDRY and its potential importance for *Plasmodium* infections, and identify a putative, novel X-linked chromosomal inversion in GOUNDRY that may be a barrier to gene flow with closely related subgroups. We discuss these results in the context of malaria control efforts.

Materials and Methods

Mosquito samples

Mosquito sample collection and species/subgroup identification was previously described for *A. coluzzii,* GOUNDRY, and *A. arabiensis* samples (Riehle *et al.* 2011).

Briefly, larvae and adults were collected from three villages in Burkina Faso in 2007 and 2008 (Table S1). Larvae were reared to adults in an insectary, and both field caught adults and reared adults were harvested and stored for DNA collection. In addition to standard species diagnostic assays, individuals were assigned to genetic subgroups using genetic clustering analysis based on 3rd chromosome SNPs and microsatellites (Riehle *et al.* 2011). One *A. gambiae* individual was also included in this study. This sample was collected indoors as an adult in the village of Korabo in the Kissidougou prefecture in Guinea in October 2012. Individuals were typed for species, molecular form and *2*L*a* karyotype using a series of standard molecular diagnostics (Fanello *et al.* 2002; White *et al.* 2007; Santolamazza *et al.* 2008). All *A. coluzzii* and *A. arabiensis* samples are $2La^{a/a}$ homokaryotypes and the *A. gambiae* sample typed as a heterokaryotype ($2La^{a/+}$). As discussed above, both forms of the 2La inversion are segregating in GOUNDRY, and we chose to sequence eleven $2La^{+/+}$ GOUNDRY samples and one $2La^{a/a}$ sample (GOUND_0446).

DNA extractions, genome sequencing, short-read processing

A detailed description of the DNA extractions, sequencing, and processing has been included in a separate publication (Crawford *et al.* 2015) , but briefly, genomic DNA was extracted using standard protocols and was sequenced using the Illumina HiSeq2000 platform by BGI (Shenzhen, China). Paired-end 100-bp reads were obtained for all samples. The *Anopheles gambiae* sample was sequenced on the same platform at the University of Minnesota Genomics Center core facility. Raw Illumina reads were deposited at NCBI SRA under BioProject ID PRJNA273873. Short-reads were aligned in two steps using BWA-mem (v0.7.4) alignment algorithm [(Li 2013); bio-bwa.sourceforge.net]. First, reads were mapped to the *A. gambiae* PEST AgamP3 reference assembly [(Holt *et al.* 2002); vectorbase.org]. Second, reads were mapped to a new updated sequence where the major allele (frequency in sample ≥ 0.5) from each population were substituted into the PEST reference to make population specific references. Local realignment around indels was conducted with GATK v.2.5-2 (DePristo *et al.* 2011). Duplicates were removed using the SAMtools v.0.1.18 (Li *et al.* 2009) *rmdup* function. We applied a series of quality filters and identified a set of robust

genomic positions that were included in all downstream analysis. As a rule, heterochromatic regions as defined for *A. gambiae* (Sharakhova *et al.* 2010) were excluded from all analyses since short read mapping is known to be problematic in such regions.

Bioinformatics and population genetic analyses

Detailed descriptions of additional methods, mostly involving standard approaches and previously existing software, can be found in Appendix S1. Included are descriptions of genotype calling, estimation of nucleotide diversity, fixed difference calling, calculation of genetic divergence (D_{xy}) and the neighbor-joining tree, ancestral sequence synthesis, demographic model inference, selective sweep dating, and putative inversion breakpoint mapping.

Inbreeding analysis

Estimating inbreeding coefficients

Initial estimates of the global site frequency spectrum (SFS) in GOUNDRY produced distributions of allele frequencies that deviated substantially from standard equilibrium expectations, as well as from those observed in the *A. coluzzii* and *A. arabiensis* groups. Most notably, the proportion of doubletons was nearly equal to that of singletons in *A. gambiae* GOUNDRY (see Results). This observation is consistent with widespread inbreeding in the GOUNDRY subgroup. We tested the hypothesis of extensive inbreeding in two ways, with the goals of both characterizing the pattern of inbreeding in this subgroup as well as obtaining inbreeding coefficients for each individual that could then be used as priors for an inbreeding-aware genotype-calling algorithm. We used the method of Vieira et al. (Vieira *et al.* 2013), which estimates inbreeding coefficients in a probabilistic framework taking uncertainty of genotype calling into account. This approach is implemented in a program called ngsF (github.com/fgvieira/ngsF). ngsF estimates inbreeding coefficients for all individuals in the sample jointly with the allele frequencies in each site using an Expectation-Maximization (EM) algorithm (Vieira *et al.* 2013). We estimated minor allele frequencies at each site (-doMaf 1) and defined sites as variable if their minor allele

frequency was estimated to be significantly different from zero using a minimum log likelihood ratio statistic of 24, which corresponds approximately to a *P* value of 10^{-6}. Genotype likelihoods were calculated at variable sites and used as input into ngsF using default settings. For comparison, we estimated inbreeding coefficients for *A. coluzzii*, GOUNDRY, and *A. arabiensis* using data from each chromosomal arm separately.

Recalibrating the site-frequency spectrum and genotype calls

We used the inbreeding coefficients obtained above for the GOUNDRY sample as priors to obtain a second set of inbreeding-aware genotype calls and an updated global SFS. We used ANGSD v.0.534 to make genotype calls as described above. However, in this case, we used the –indF flag within ANGSD, which takes individual inbreeding coefficients as priors instead of the global SFS (Vieira *et al.* 2013). Similarly, we used the inferred inbreeding coefficients to obtain an inbreeding-aware global SFS. We estimated the global SFS from genotype probabilities using –realSFS 2 in ANGSD, which is identical to –realSFS 1 (Nielsen *et al.* 2012) except that it uses inbreeding coefficients as priors for calculations of posterior probabilities (Vieira *et al.* 2013).

IBD Tracts

We examined the effects of inbreeding within diploid individuals using FEstim (Leutenegger *et al.* 2006, 2011), which implements a maximum likelihood method within a Hidden-Markov-Model that models dependencies along the genome. We used the FSuite v.1.0.3 (Gazal *et al.* 2014) pipeline to generate submaps, estimate inbreeding parameters using FEstim, identify IBD tracts, and plot IBD tracts using Circos v.0.67-6 (Krzywinski *et al.* 2009). To minimize linkage disequilibrium that creates non-independence among SNPs while maximizing information content, we generated 20 independent random subsets of between 187 and 193 SNPs (or submaps) spaced at least 1 kb apart, and inbreeding parameters were inferred using all 20 submaps. We used allele frequencies estimated using ANGSD above (-doMaf and -indF) for calculation of emission probabilities in FEstim. We also used genetic maps for *Anopheles gambiae* from Zheng et al. (Zheng *et al.* 1996). To convert data from Zheng et al. to dense genetic maps, we mapped primers from that study onto the *Anopheles gambiae* PEST

reference using standard e-PCR approaches that map PCR primers onto a reference sequence using computational sequence matching. Autosomal maps and code for polynomial analysis were kindly provided by Russ Corbett-Detig (github.com/tsackton/linked-selection/), and we performed e-PCR mapping for the X chromosome. We fit a polynomial function to the genetic map for each chromosome and used this function to convert the physical position of SNP marker to genetic distance. For this analysis, we joined the left and right arms of chromosomes 2 and 3 by adjusting the physical position of SNPs on the left arms by the full length of the right arm.

FSuite is designed for genotyping array data and does not allow any genotyping errors. Therefore, we took additional steps to minimize the effects of genotyping errors. First, we set a minimum minor allele frequency of 10% and included only genotypes with 95% posterior probability. Second, we set a liberal threshold of $1e^{-6}$ for the minimum posterior probability required for considered IBD. Since this threshold allows many small IBD tracts that are likely to be erroneous, we set a minimum size threshold of 0.1 cM for inclusion in the final set of IBD tracts.

Ruling out bioinformatic and sequencing artifacts

Since the observation of high rates of inbreeding stem directly from intermediate coverage (~10X) next-generation sequencing data that can be prone to bioinformatic errors and biases, we conducted several tests to determine whether such artifacts could explain the observed inbreeding signal. One possible artifact could stem from mapping or alignment biases against divergent next-generation reads that could lead to excess homozygosity. If mapping is unbiased, the proportion of reference bases at heterozygous sites should be distributed with a mean of 0.5. We find that the mean proportion of reference bases at heterozygous sites is 0.4893 ($\sigma = 0.1646$) in *A. coluzzii* and 0.4757 ($\sigma = 0.1581$) in GOUNDRY indicating very similar read distributions in these populations (Figure S1). Although both populations show a small deviation from 0.5 at biallelic sites, this deviation cannot explain large regions of homozygosity in GOUNDRY.

We also asked whether excess homozygosity could stem from erroneous assignment of homozygous genotypes at true heterozygous sites. Such errors could result if short read depths were exceptionally low in some genomic regions. We calculated read

depths at sites in different genotype classes in GOUNDRY and find that the mean read depth is 12.3569 (σ = 5.3917) at homozygous reference sites, 12.2156 (σ = 5.1235) at homozygous alternative sites, and 12.6871 (σ = 5.5163) at heterozygous sites, indicating that the distribution of read depth is very similar between all three classes (Figure S2). We find a similar pattern in *A. coluzzii*, which shows no evidence of inbreeding. In this population, the mean read depth is 10.4773 (σ = 4.7555) at homozygous reference sites, 11.0082 (σ = 4.1849) at homozygous alternative sites, and 10.6660 (σ = 4.7755) (Figure S2). Moreover, the distributions of read depths at heterozygous sites and homozygous sites are very similar in both the *A. coluzzii* and GOUNDRY populations (Figure S2). These results strongly suggest that bioinformatic artifacts cannot explain the excess homozygosity and IBD tracts observed in GOUNDRY.

Large variations in observed sequence diversity could also stem from issues related to DNA sequencing. Importantly, the same DNA preparation and library preparation protocols were used for GOUNDRY as well as *A. coluzzii* and *A. arabiensis*, so the increased IBD observed in GOUNDRY is not likely attributable to a difference in sample preparation. Low DNA input could also lead to artifacts in sequencing, but the total mass of DNA used for library preparation did not differ between GOUNDRY and the other samples that were all sequenced together (Table S1). In general, DNA mass and handling was similar between GOUNDRY and the other populations examined here that do not harbor long IBD tracts, suggesting that such differences cannot explain the signals of increased inbreeding in GOUNDRY.

Inbreeding-phenotype association test

Since 12 GOUNDRY genomes is not a large enough sample size for association testing, we obtained SNP genotype data for 274 GOUNDRY individuals who had also been phenotyped in a *Plasmodium* infection experiment as part of an independent study (Mitri *et al.* 2015). Full details of Illumina SNP chip assay design and data collection and infection experiments are available in that publication but will be summarized here. Briefly, larvae were collected in three villages in central Burkina Faso, and raised to

adulthood in the laboratory where females were given *Plasmodium falciparum*-infectious bloodmeals from local volunteers. Fully fed females were dissected 7-8 days later for oocyst quantification and DNA extraction. For the Illumina SNP chip, SNPs were identified from raw sequence reads generated for genome sequencing projects for *A. coluzzii* and *A. gambiae* as well as from independent deep sequencing efforts. DNA hybridization and genotype calling were conducted using standard procedures followed by stringent quality filtering of genotype calls and independent confirmation using duplicate hybridizations and independent Sequenom assays using a subset of SNPs. We used a set of SNPs distributed approximately uniformly across the autosomes. Among these sites, we included only sites (n = 678) that were variable in the GOUNDRY subgroup.

We used ngsF (Vieira *et al.* 2013) to estimate inbreeding coefficients for each of the 274 females using the SNP genotype data as input. Since genomic estimates of inbreeding coefficients are statistically noisy with less than 1000 SNPs, we used a bootstrap approach by sampling the SNPs with replacement to make 1000 new bootstrapped datasets of the same size, estimating inbreeding coefficients using ngsF. Point estimates of the inbreeding coefficients were obtained by taking the mean of log 10 transformed bootstrap values and re-transforming the mean value.

To test whether infection prevalence was higher in inbred individuals, we used a two-by-two χ^2 test . The table cells corresponded to 'infected' and 'not infected' phenotypes as well as high and low inbreeding coefficients. Since the distribution of inbreeding coefficients was not bimodal, we categorized individuals as either 'high' or 'low' inbreeding levels based on whether their inbreeding coefficient was above or below a cutoff value, respectively. We included two cutoff values: 1) F = the median coefficient value of 0.026, and 2) The maximum F estimated from genome sequencing in *A. coluzzii*, which does not show signs of inbreeding. To establish statistical significance while preserving correlations among mosquitoes within each blood donor cohort, we randomly permuted infection phenotype among mosquitoes within donor cohort, and recalculated the χ^2 value. We compared the empirical χ^2 value to 10^4 values from permuted datasets in a one-tailed statistical test. We further tested the association and the effect of blood-donor using the Cochran-Mantel-Haenszel procedure (cmh.test in R)

that directly accounts for additional factors within the contingency test. To test for correlations between inbreeding coefficients and the number of oocysts (infection intensity), we fit a linear model to relate inbreeding coefficients (log transformed) to the number of oocyts (log transformed) with blood-donor as a factor in the model. Only mosquitoes with at least one oocyst were included in this part of the analysis.

Results

Genome Sequencing and Population Genetic Analysis

We have completely sequenced the genomes of 12 field-captured female *Anopheles* GOUNDRY mosquitoes from Burkina Faso and Guinea using the Illumina HiSeq2000 platform. We compared these genomes to full genomes from *A. coluzzii* (n=10), *A. gambiae* (n=1) and *Anopheles arabiensis* (n=9). Most individuals were sequenced to an average read depth of 9.79x, while one individual each from GOUNDRY, *A. coluzzii*, and *A. gambiae* was sequenced to at least 16.44x (Table S1). We also used publicly available genome sequences from *Anopheles merus* (*Anopheles gambiae* 1000 Genomes Project) as an outgroup. We conducted population genetic analysis of aligned short-read data using genotype likelihoods and genotype calls calculated using the probabilistic inference framework ANGSD (Korneliussen *et al.* 2014).

Genetic Relatedness Among Species and Subgroups

To determine the genetic relationship of the GOUNDRY subgroup to other known species and subgroups of *Anopheles*, we calculated an unrooted neighbor-joining tree based on genome-wide genetic distance (D_{xy}) at intergenic sites (Figure 1). Previous findings indicated that the recently discovered GOUNDRY subgroup of *A. gambiae* is a genetic outgroup to *A. coluzzii* (formerly known as M molecular form) and *A. gambiae* (formerly S form) (Riehle *et al.* 2011). However, our data indicate that GOUNDRY is actually genetically closer to *A. coluzzii* (D_{GAc} = 0.0109; 100% bootstrap support) than either group is to *A. gambiae* (D_{GAg} = 0.0149; D_{AcAg} = 0.0143).

It has been speculated that GOUNDRY may be a recently formed backcrossed hybrid of *A. coluzzii* and *A. gambiae* (Lee *et al.* 2013). This hypothesis also predicts that

GOUNDRY will be segregating chromosomes that are mosaics of haplotypes derived from *A. coluzzii* and *A. gambiae*, and therefore most, if not all, polymorphisms found in GOUNDRY should also be found in one of these putative parental taxa. In contrast, we find 7,383 fixed differences between *A. coluzzii* and GOUNDRY [excluding 2L since it is dominated by the large 2L*a* inversion known to have crossed species boundaries (Fontaine *et al.* 2015)], of which 27% are putatively GOUNDRY-specific alleles not shared with *A. gambiae*, *A. arabiensis*, or *A. merus*. GOUNDRY shares an allele with the *A. gambiae* individual sampled here at an additional 31.5% of the fixed sites, although this number may increase if more *A. gambiae* samples are included. These results do not exclude the possibility of gene flow between GOUNDRY and *A. gambiae*, but they fail to support the hypothesis that GOUNDRY is simply a very recent hybrid of *A. coluzzii* and *A. gambiae*. Instead, the substantial number of putatively GOUNDRY-specific fixed alleles support GOUNDRY as a unique subgroup that may have originated as an offshoot of *A. coluzzii* and experienced subsequent gene flow from *A. gambiae.*

Origins of GOUNDRY

It has been hypothesized that the advent of agriculture in sub-Saharan Africa ~5-10 kya played a role in driving diversification and expansion of *Anopheles* mosquitoes (Coluzzi *et al.* 2002). The two-dimensional site-frequency spectrum reveals substantial differentiation in allele frequencies between GOUNDRY and *A. coluzzii* with many fixed differences differentiating these groups and is not compatible with a very recent origin of GOUNDRY (Figure 2). To test whether the origin of GOUNDRY could have been associated with habitat modification driven by agriculture, we fit four population historical models with increasing complexity (Figure 2; Table 1; Methods) to the two-dimensional site frequency spectrum for GOUNDRY and *A. coluzzii* using *dadi* (Gutenkunst *et al.* 2009). The 2D spectra from the empirical data and the best-fit model for each demographic model are presented in Figure 2. We first fit a simple one-epoch, split model with no migration. The maximum-likelihood model under this scenario gave a poor fit to the empirical data with a likelihood value (*L*) of -176,635.8. We then added asymmetrical migration to the model (one-epoch, split with migration), which resulted in a nearly three-fold improvement of the likelihood value improvement of the fit of the

model to the data with $L_{1\text{-ep-splt-mig}}$ = -59.896.75 -, providing strong evidence that migration has played a key role in the history of these taxa. Residual differences between the 2D spectra from the model and the data (Figure 2), however, were unevenly distributed across the spectra, suggesting that one-epoch models are missing potentially important features of the demographic history. To improve flexibility in the model fitting, we fit both two-epoch and three-epoch population split-with-migration models (Table 1). Interestingly, the adding a second epoch did not result in a substantial improvement of the fit to the data as indicated by the remaining large residuals and decreased likelihood value ($L_{2\text{-ep-splt-mig}}$ = -59,949.49) relative to the one-epoch model. Adding a third epoch, however, achieved a considerable improvement of the fit to the data ($L_{3\text{-ep-splt-mig}}$ = -49,023.85). Residuals indicating differences between the model and data are also presented and suggest that deviations between spectra associated with the model and data are well correlated.

The best-fitting three-epoch-split-with-migration model (Table 1) predicts that these subgroups diverged ~111,200 ya (95% CI 96,718 – 125,010), followed by a 100-fold reduction in the size of both subgroups after isolation (Methods). The timing of this model rejects any role of modern agriculture in subgroup division, although it should be noted that estimates of such old split times inherently carry considerable uncertainty. Our inferred model is inconsistent by an order of magnitude with agriculture as a driving force in cladogenesis and is more consistent with habitat fragmentation and loss due to natural causes, potentially including climatic shifts such as changes in pluviometry that would lead to increased population size. The model supports a >500-fold population growth in *A. coluzzii* and 19-fold growth in GOUNDRY with extensive gene flow between them ~85,300 ya, consistent with a re-establishment of contiguous habitat and abundant availability of bloodmeal hosts. Interestingly, the model supports additional population growth in both subgroups in the most recent epoch, which spans the last 10,000 years and coincides with the advent of agriculture. Any hybridization related to secondary contact during this period has not led to complete homogenization, as we conservatively identified nearly 8,000 fixed nucleotide differences distributed across the genomes of the two subgroups.

The dates reported here depend on assumptions about both the physiological mutation rate as well as the number of generations per year, neither of which are well known in *Anopheles*. As such, the details of these results would differ somewhat if different estimates were used. However, we would have to invoke extreme values of these parameters that are outside reasonable expectation in order to obtain estimates for the time of the GOUNDRY- *A. coluzzii* split that coincides with the advent of agriculture. Overall, the model suggests that the origin of GOUNDRY is not recent and both GOUNDRY as well as *A. coluzzii* have both undergone bouts of population growth and increased rates of hybridization in more recent evolutionary time.

The initial description of GOUNDRY (Riehle *et al.* 2011) suggested that it harbored lower allelic diversity than other sampled subgroups potentially suggesting a small effective population size while being proportionally more numerous than other subgroups at the time and place of collection. Our model suggests that the recent effective population size is approximately 98,400 (95% CI 55,100 – 158,500) compared to a recent *A. coluzzii* effective size of approximately 1,558,000 (95% CI 848,000 – 2,508,000). The disparity between recent effective sizes of these two subgroups suggests that, while GOUNDRY may have been locally abundant at the time and place of the initial study, it is not likely to be geographically widespread on a scale similar to *A. coluzzii*.

Novel X-linked chromosomal inversion in GOUNDRY

A large cluster of fixed differences (~ 530; Figure S3) identified between GOUNDRY and *A. coluzzii* falls within a 1.67 Mb region on the X chromosome that is nearly absent of polymorphism (Figure 3), despite sequence read coverage comparable to neighboring genomic regions (Figure S3). The remarkably large size of the region devoid of diversity would imply exceptionally strong positive selection under standard rates of meiotic recombination. For comparison, previously identified strong sweeps associated with insecticide resistance span approximately 40 Kb and 100 kb in freely recombining genomic regions of *Drosophila melanogaster* and *D. simulans,* respectively (Schlenke & Begun 2004; Aminetzach *et al.* 2005). The swept region in GOUNDRY is marked by especially sharp edges (Figure 3), implying that recombination has been

suppressed at the boundaries this region. Collectively, these observations suggest that the swept region may be a small chromosomal inversion, which we have named X*h* in keeping with inversion naming conventions in the *Anopheles* system. Notably, this pattern is virtually identical to the pattern of diversity in a confirmed X-linked inversion discovered in African populations of *D. melanogaster* (Corbett-Detig & Hartl 2012). The X*h* region in GOUNDRY includes 92 predicted protein coding sequences (Table S2), including the *white* gene, two members of the gene family encoding the TWDL cuticular protein family (*TWDL8* and *TWDL9*), and five genes annotated with immune function (*CLIPC4, CLIPC5, CLIPC6, CLIPC10, PGRPS1*). The lack of diversity in the region implies that the presumed X*h* inversion has a single recent origin and was quickly swept to fixation in GOUNDRY. We estimated the age of the haplotype inside the sweep region to be 78 years with a standard deviation of 9.15 by assuming that all segregating polymorphisms in the region postdate fixation of the haplotype (see Methods). Such extraordinarily recent adaptation is consistent with the selection pressures related to 19th and 20th century human activity such as insecticide pressure or widespread habitat modification.

Xh is a barrier to introgression

Chromosomal inversions are thought to play important roles as barriers to gene flow between taxa diverging with ongoing gene flow (Rieseberg 2001; Noor *et al.* 2001; Navarro & Barton 2003), so we hypothesized that this putative X-linked chromosomal inversion in GOUNDRY may serve as a barrier to gene flow with *A. coluzzii*. If this inversion has acted as a barrier to gene flow with *A. coluzzii,* or taxa undergoing secondary contact after divergence, we would expect the X chromosome to be more diverged than the autosome and the inversion would be more diverged than other regions of the X chromosome.

One approach to estimate differences in divergence among genomic regions is to compare divergence between a focal pair of subgroups (GOUNDRY and *A. coluzzii*) to divergence between one of the focal groups and an outgroup (GOUNDRY and *A. gambiae*) in order to scale divergence levels by differences among regions in mutation rate and the effects of selection on linked sites. This approach estimates what is known

as Relative Node Depth (RND = D_{GAc}/D_{GAg}, where subscripts G, *Ac*, and *Ag* indicate GOUNDRY, *A. coluzzii*, and *A. gambiae* respectively), and a higher RND indicates greater divergence between the focal groups (Feder *et al.* 2005). We find that RND is 0.7797 on the autosomes and 0.8058 on the X, indicating higher genetic divergence between GOUNDRY and *A. coluzzii* on X relative to the autosomes. To explicitly test whether such a pattern could be obtained under a pure split model with no gene flow, we obtained expected values of Relative Node Depth (RND) assuming a phylogeny where *A. coluzzii* and GOUNDRY form a clade with *A. gambiae* as the outgroup (Methods).

Our analytical results support the hypothesis that D_{GAc} is downwardly biased on the autosomes relative to D_{GAc} on the X as a result of higher rates of gene flow on the autosomes relative to the X. We find that under some parameter combinations (Figure 4), RND decreases with increasing effective *A.coluzzii* -GOUNDRY effective population size, which could result in a smaller RND value on the autosomes since the autosomes should have an effective size at least as big as the X. However, most parameter combinations suggest that this pattern is unexpected (i.e. most regions of the curves predict that RND should increase with increasing effective population size), and the estimate for the ancestral effective size of *A.coluzzii*-GOUNDRY we obtained in a separate demographic analysis above suggests that these subgroups exist in a parameter space where the RND function is consistently increasing with increasing effective sizes.

To test the second expectation that the inversion is more diverged than other regions on the X chromosome, we compared divergence with *A. coluzzii* in windows inside and outside of the inverted region. Absolute sequence divergence (D_{xy}) is not sensitive to detect differential gene flow for relatively recent changes in gene flow (Cruickshank & Hahn 2014), and we expect that the putative X*h* inversion is likely too young for measurable differences to have accumulated, so we tested for excess divergence in the X*h* inversion using a more sensitive approach. For comparison, we find that the inverted region is significantly more diverged between *A. coluzzii* and GOUNDRY relative to the remaining X chromosome ($\overline{D}_{GAc}$ (X*h*) = 0.0103, $\overline{D}_{GAc}$ (non-X*h*) = 0.0071; M-W $P < 2.2\times10^{-16}$), but nucleotide diversity in *A. coluzzii* is also significantly higher in this region (π_{Ac} (X*h*) = 0.0080, π_{Ac} (non-X*h*) = 0.0061; M-W $P < 5.49\times10^{-14}$), implying that the increased divergence could be partially explained by

494 increased mutation rate in this region. However, when absolute divergence along the X
495 chromosome is explicitly scaled by the mutation rate inferred from levels of
496 polymorphism in the *A. coluzzii* sample (D_a), the putatively adaptive X*h* inversion
497 between GOUNDRY and *A. coluzzii* is proportionally much more divergent than is the
498 remainder of the X chromosome ($\overline{D}_a$ (X*h*) = 0.0022, $\overline{D}_a$ (non-X*h*) = 0.0013; M-W $P <$
499 4.89×10^{-08}; Figure 5). Although relative measures of divergence, such as D_a, are known,
500 for example, to be confounded by reductions in nucleotide diversity related to natural
501 selection on linked sites (Charlesworth 1998; Noor & Bennett 2009), we believe that this
502 analysis is robust to these concerns because the comparison is among only X-linked
503 windows and the region of interest is in a region of the chromosome that is highly diverse
504 in subgroups where there is no evidence of selective sweeps (Figure 3).
505 Both of these tests indicate that sequence divergence between *A. coluzzii* and
506 GOUNDRY is greater inside the putative inversion relative to the X as a whole, which
507 likely reflects both the accumulation of a small number of new private mutations inside
508 the inversion as well as a greater proportion of shared polymorphisms outside the
509 inversion, consistent with higher rates of introgression outside the inversion. Taken
510 together with the demographic inference, the above results suggest that, after initial
511 ecological divergence between these taxa approximately 100,000 years ago, this genomic
512 barrier to introgression has established in the face of ongoing hybridization only within
513 the last 100 years, presumably owing to the accumulation and extended effects of locally
514 adapted loci or genetic incompatibility factors within the large swept/inverted X*h* region
515 on the GOUNDRY X chromosome, meiotic drive, or aneuploidy resulting from
516 nondisjunction in heterokaryotypes.
517
518 ***GOUNDRY is inbred***
519 Unexpectedly, we found that GOUNDRY exhibits a deficiency of heterozygotes
520 relative to Hardy-Weinberg expectations and extensive regions of Identity-By-Descent
521 (IBD), a pattern that is not observed in any of our other *Anopheles* collections. Individual
522 diploid GOUNDRY genomes are checkered with footprints of IBD, even though the
523 genome as a whole harbors substantial genetic variation indicating a relatively large
524 genetic (effective) population size (Figure 6a). The observation of stochastic tracts of

IBD is most consistent with an unusually high rate of close inbreeding. To explicitly test for elevated inbreeding coefficients (*F*), we used a maximum likelihood framework to infer *F* for each individual without calling genotypes. We found that values of *F* range from 0.0087 to 0.2106 genome wide (Figure S4). In contrast, estimates of inbreeding coefficients for 10 *A. coluzzii* genomes and 9 *A. arabiensis* genomes were consistently low ($F_{Ac} < 0.03$; $F_{Aa} < 0.04$). The relatively high inbreeding coefficients in GOUNDRY suggest that this population has a history of mating among relatively closely related individuals.

The lengths of these tracts provide information about the timing and nature of inbreeding in the population since recombination is expected to break up large tracts generated by recent inbreeding. All 12 GOUNDRY genomes analyzed here are marked by IBD tracts of various lengths, and the specific chromosomal locations of the IBD regions are random and vary among the sequenced GOUNDRY individuals (Figure 6b). While many IBD tracts are relatively short, several individuals harbor tracts that span 30-40 cM (Figure 6c). This mixture of tract lengths is most consistent with both a generations-old history of inbreeding (short tracts) as well as the possibility of mating among half-siblings or first-cousins (long tracts).

Effect of inbreeding on* Plasmodium-*resistance

Inbreeding is known to have detrimental effects on various phenotypes, including resistance to parasite infection (Hamilton *et al.* 1990; Luong *et al.* 2007). To test whether inbreeding in GOUNDRY increases intrinsic susceptibility to *Plasmodium falciparum* infection in this group, we studied a larger panel of 274 GOUNDRY females that were experimentally infected with local wild isolates of *P. falciparum* and genotyped at 1,436 SNPs across the genome (Mitri *et al.* 2015). After filtering, we estimated inbreeding coefficients with the program *ngsF* (Vieira *et al.* 2013) using 678 autosomal variable sites (Methods) and found that *F* ranges from 0 to 0.3797 in this sample of GOUNDRY females (Figure S5). Although it is possible that some GOUNDRY individuals are truly not inbred, all 12 GOUNDRY individuals subjected to whole genome sequencing showed significant evidence of inbreeding, so we suspect that the relatively sparse genotyping (1

per ~400 kb) assay used on this panel of mosquitoes failed to capture IBD tracts in some individuals.

Blood feeding experiments were conducted using five human *Plasmodium* gametocyte donors, and blood donor had a significant effect on both infection prevalence (ANOVA; $P = 1.593\times10^{-9}$) and intensity (ANOVA; $P = 1.194\times10^{-13}$). Importantly, the distributions of mosquito inbreeding coefficients did not differ significantly between blood donor cohorts (ANOVA, $P = 0.0934$).

Of the females that fed on infectious blood-meals, 104 (37.9%) had no parasites at the time of dissection, and we asked whether this infection prevalence is statistically associated with inbreeding in the mosquito host. Inspection of the distribution of F in this sample indicates that categorization of individuals as inbred or outbred is difficult since a substantial proportion of individuals were assigned values of F close to 0 (Figures S5 and S6) and even individuals from outbred populations such as *A. coluzzii* and *A. arabiensis* can have estimates of F as high as 0.03 or 0.04 (Figure S4). Therefore, we used the median value of F estimated from genome-wide SNPs in GOUNDRY (0.026) and categorized mosquitoes as more inbred ($F > 0.026$) or less inbred ($F \leq 0.026$). We used a χ^2 test with this categorization approach to test whether higher inbreeding significantly associated with higher infection prevalence and find that females with higher inbreeding coefficients are overrepresented in the 'infected' class ($P = 0.0205$; Table 2). We also used the Cochran-Mantel-Haenszel procedure to directly account for blood-donor in the test for association and found very similar results ($P = 0.025$ for median cutoff). As an alternative assignment approach, we defined the inbreeding categories using the highest inbreeding coefficient value obtained from full genome sequencing of an outbred population, *A. coluzzii* ($F = 0.0292$), which should be more robust to statistical uncertainty than estimates from the SNP chip data, and find that the association is on the borderline of significance ($P = 0.0546$; Table 2). These analyses indicate that an increase in the proportion of genes with alleles that are Identical by Descent may decrease the ability of adult female mosquitoes to resist parasite infection, although the effect is small enough that detection of the association is sensitive to how the distribution of F is categorized.

We also asked whether the degree of inbreeding has an effect on the intensity of infection (number of oocysts per midgut). Of the 274 females that fed on natural gametocytemic blood samples and were assayed for infection status, 170 harbored at least one oocyst, while the remaining 104 females were uninfected, corresponding to an infection rate of 0.62. Among the infected females, infection intensity varied from 1 to 38 with a mean of 5.73 oocysts per individual. We fit linear models for mosquitoes fed on each blood donor separately and find no significant correlation ($P > 0.05$) between inbreeding coefficients and infection intensity.

Discussion

It is not known how many such cryptic subpopulations of *Anopheles* exist or how much gene flow they share with described subgroups, although there is evidence gene flow may be common (Lee *et al.* 2013). Epidemiological modeling and vector-based malaria control strategies must account for populations like GOUNDRY if they are to effectively predict disease dynamics and responses to intervention (Griffin *et al.* 2010). Failure to account for such subpopulations will undermine malaria control efforts, as in the case of the Garki malaria control project in Nigeria in the 1970s that did not account for genetic variation in adult resting behavior and missed outdoor resting adults (Molineaux *et al.* 1980) .

Here, we present an analysis of complete genome sequences from the newly discovered cryptic GOUNDRY subgroup of *A. gambiae*. Our results help clarify some outstanding questions raised by the initial description of this subgroup. We show that, in contrast to initial suggestions (Riehle *et al.* 2011), GOUNDRY subgroup of *A. gambiae* falls genetically within *Anopheles gambiae sensu lato* and is not an outgroup. GOUNDRY shows strongest genetic affinity with *A. coluzzii* and therefore may be an ecologically specialized subgroup of *A. coluzzii*. The discrepancy between our findings and previously published results is likely due to the fact that the first description was based on a small number of microsatellite markers and SNPs and was based on differences in allele frequency, while the current study is based on absolute sequence divergence calculated from whole genome sequencing data, and therefore included both shared and private mutations. Our demographic analysis suggests that GOUNDRY has

existed for approximately 100,000 years and represents a recent example of the frequent speciation dynamics in *Anopheles* that appears to be common (Crawford *et al.* 2015; Fontaine *et al.* 2015). Since GOUNDRY was identified using an outdoor sampling approach not common in previous studies, it was unclear whether or not this subgroup may be more broadly distributed and just un-sampled. We estimate that the recent (effective) population size of GOUNDRY is approximately 5% that of *A. coluzzii*, suggesting that GOUNDRY is likely restricted to a relatively small region of the Sudan-Savanna zone in West Africa.

In addition to thousands of mutations found to be putatively unique to GOUNDRY, we identified a large GOUNDRY-specific genetic marker in the form of a new putative X-linked chromosomal inversion that originated and fixed within GOUNDRY within the last 100 years. It remains unknown whether positive selection or meiotic drive has driven this inverted haplotype to high frequency and ultimately fixation in GOUNDRY, but our results suggest that it may serve as a recent barrier to gene flow with *A. coluzzii*, and potentially other taxa as well. Collectively, the data show that nucleotide-diversity corrected divergence is higher inside the putative inverted region, the inverted region as a chromosomal segment is the most diverged of all segments of the same size on the X chromosome, and the X chromosome as a whole is more diverged among GOUNDRY and *A. coluzzii* relative to the autosomes. The most parsimonious explanation for these patterns is that, although very few new mutations have accumulated inside of X*h* since its origin less than 100 years ago, ongoing gene flow between *A. coluzzii* and GOUNDRY has led to a greater density of shared polymorphism and therefore lower sequence divergence in non-inverted regions of the X chromosome relative to the inversion, especially distal to the inversion breakpoints. These results lead us to conclude that while cladogenesis of GOUNDRY and *A. coluzzii* ~100 kya by other means established some degree of temporally fluctuating reproductive isolation, the recently derived X*h* putative inversion now serves as a genomic barrier to gene flow, and the effects of selection against migrant haplotypes or lack of recombination with non-inverted chromosomes have begun to extend to linked sites outside the inversion breakpoints.

The observation that GOUNDRY is more closely related at the genome level to *A. coluzzii* than to *A. gambiae* could be biased by higher rates of gene flow between GOUNDRY and *A. coluzzii* as well as sampling bias caused by the fact that *A. gambiae* is represented by only a single individual that was sampled from a different country. Although we cannot formally rule out the possibility that GOUNDRY originated as something other than a subpopulation of *A. coluzzii* and later experienced substantial gene flow from *A. coluzzii* that led to genetic affinity in our analysis, the most parsimonious explanation is that it is a subgroup that originated from *A. coluzzii* that has experienced gene flow from multiple sympatric taxa over its history. The most compelling piece of evidence that GOUNDRY is not a recent *A. coluzzii-A. gambiae* hybrid-backcross is the presence of the large fixed haplotype on the X chromosome in GOUNDRY that is not expected under the recent backcross model. In support of this notion, a recently published study (Fontaine *et al.* 2015) constructed similar distance based trees using samples of *A. gambiae* from across the continent and found that geographically disparate individuals were consistently interdigitated while excluding *A. coluzzii*, suggesting that species assignment was more important than geography.

An additional potential concern regarding our estimate of the demographic modeling and our conclusion that the X chromosome is more diverged than the autosome between GOUNDRY and *A. coluzzii* stems from introgression between *A. gambiae* and both GOUNDRY and *A. coluzzii*. We showed in a companion manuscript that GOUNDRY has introgressed with *A. gambiae* in the evolutionarily recent past (Crawford *et al.* 2015), and the presence of *A. gambiae* haplotypes in GOUNDRY could bias our demographic estimate of the split time since this introgression was not explicitly modeled. A four-taxon model including *A. gambiae* and *A. arabiensis* would probably improve our estimates, but the dimensionality of such a model would increase dramatically and would require much more sequence data than is available in the current study. Introgression with *A. gambiae* could also compromise our RND analysis in which this group was used as an outgroup. For example, higher introgression between *A. gambiae* and the ingroups on the X relative to the autosome could result in an underestimate of the mutation rate on the X chromosome and thus an inflation of the ingroup divergence. However, we showed in a companion manuscript (Crawford *et al.* 2015) that signals of introgressed haplotypes

677 are concentrated on the autosome and absent from the X, suggesting that RND scaling
678 may be downwardly biased on the autosomes rather than the X. For these reasons, *A.*
679 *gambiae* is not an ideal outgroup for an RND analysis, but it is suitable for our purposes
680 and a low rate of introgression from this taxon is not likely to bias our results.
681 Perhaps the most unexpected feature of GOUNDRY is the high degree of
682 inbreeding in this population. We emphasize that the deficit of heterozygosity and
683 presence of unusually long IBD tracts that we observe in GOUNDRY are not a typical
684 function of persistently small population size. The inbreeding that we see here is
685 different from the strong drift that would be associated with small effective population
686 sizes over many generations, and which would manifest as generally low levels of
687 nucleotide diversity across the genome. Instead, the observed pattern indicates that some
688 proportion of individuals in an otherwise relatively large population tend to mate with
689 closely related individuals. Although IBD patterns in GOUNDRY are not consistent with
690 a long term small population size, in principle it could reflect a very recent and severe
691 reduction in population size, perhaps related to a strong insecticide pressure. The full
692 insecticide resistance profile of GOUNDRY is unknown. It was shown previously that a
693 resistance allele at *kdr* is segregating in this population (Riehle *et al.* 2011), although the
694 resistant and susceptible alleles are segregating at HWE, and the *kdr* allele is segregating
695 at a similar frequency in our sample (Table S1). This suggests that this locus has not
696 been subject to recent severe selection pressure in GOUNDRY.
697 We propose four hypotheses to explain the inbreeding signal in GOUNDRY.
698 Two hypotheses involve the evolution of modified mating biology where GOUNDRY
699 individuals 1) have preference for mating with related individuals, or 2) mate
700 immediately after eclosion. Two additional hypotheses involve the spatial distribution of
701 mating where GOUNDRY individuals either return to their larval habitat to mate or
702 suitable habitats are rare so they return to the same habitat by necessity. In both
703 scenarios, GOUNDRY would exist as a series of micro-populations, perhaps related to
704 habitat fragmentation, where the likelihood of mating with a related individual is higher
705 than that of larger populations such as *A. coluzzii* or *A. gambiae*. The first two
706 hypotheses are biologically less plausible and are not supported by the patterns of IBD
707 tracts since we do not observe a ‘mate preference’ locus that is inbred in all individuals or

708 uniformly long IBD tracts as predicted by these scenarios. The spatial distribution
709 hypotheses predict a distribution of mixed sized IBD tract lengths reflecting mating
710 between both close and more distant relatives by chance. Our data are consistent with the
711 spatial hypotheses, although additional field studies are needed to identify suitable
712 GOUNDRY habitat and test these hypotheses directly. Such dynamics have not been
713 previously observed in mosquito populations, which are thought to typically be large and
714 outbred.
715 Inbreeding is known to have negative fitness consequences in some cases
716 (Hamilton *et al.* 1990; Luong *et al.* 2007). Detrimental effects of inbreeding can be
717 caused either directly when individuals become homozygous for less fit alleles at a given
718 gene or indirectly when overall vigor of an individual is reduced due to exposure of
719 multiple small effect recessive mutations (Charlesworth & Charlesworth 1987). Reduced
720 immune performance is one possible effect of inbreeding, which could have implications
721 for public health if *Anopheles* mosquitoes become more effective vectors of *Plasmodium*
722 parasites. We show here that the degree of inbreeding is positively, albeit weakly,
723 associated with infection prevalence. Our results show that the odds of an individual
724 with even moderate inbreeding coefficient getting infected are 65% greater than for
725 individuals with very low inbreeding coefficients. That we observed a significant
726 association at all is surprising given the coarse and noisy estimates of both relevant
727 parameters. Experimental *Plasmodium* infections are notoriously difficult to control and
728 highly variable even among sibling females (Medley *et al.* 1993; Niare *et al.* 2002).
729 Moreover, our estimates of inbreeding coefficients are based on a relatively small number
730 of variable sites (~650), which corresponds to an average SNP density of 1 per ~400 kb.
731 Given the large number of IBD tracts that are smaller than 400 kb (Figure 6), our
732 estimates are likely to miss many smaller IBD tracts and thus be underestimates of true
733 levels of IBD within these genomes. As such, improved estimates of inbreeding may or
734 may not bolster the significant trend indicating an effect of inbreeding on infection status.
735 Inbreeding coefficients did not, however, explain variation among individuals in the
736 intensity of infection, although increasing the sample size and accuracy of the inbreeding
737 coefficients may change this conclusion. While it remains possible that our rough
738 parameter estimates inhibit this level precise correlation, a single *Plasmodium* oocyst can

be sufficient for successful transmission of the parasite. Thus, an increased odds of getting infected, regardless of how intense the infection becomes, could still have serious epidemiological consequences. More work is needed to determine the ecological and population dynamics leading to inbreeding in GOUNDRY, but it is possible that anthropogenic interventions such as intense insecticide and bed-net eradication campaigns, could in principle lead to increased inbreeding in other populations as well. Such inbreeding could be especially problematic if it causes, as our results suggest, increased efficiency in parasite transmission among the remaining small pockets of mosquitoes that escape eradication. If this is the case, the combination between the potential side effects of intense eradication efforts and ecological specialization of subgroups across time and environmental space may make complete interruption of local parasite transmission difficult.

In many ways, GOUNDRY has proven to be an atypical subgroup within the well studied *Anopheles gambiae* species complex underscoring our incomplete understanding of vector population dynamics in this system. This study has provided answers to some of the outstanding questions raised around this subgroup while generating still new questions that are difficult to reconcile. Our data suggest that GOUNDRY has existed as an offshoot population from *A. coluzzii* for many generations, hybridizing with its parental population for a substantial portion of its history, yet the most prominent genomic barrier to introgression established only very recently. The process and mechanisms that have kept these two taxa from collapsing back to a single gene pool over their history remains unclear and warrants further study. Moreover, we find evidence for a history of extensive inbreeding within GOUNDRY that we hypothesize could be explained by microstructure creating local breeding demes, yet this population is thought to be exophilic and thus likely less clustered. Whether GOUNDRY has specialized within a rare and patchy ecological niche, has become less likely to fly long distances, or has evolved in some other way that can explain this pattern remains an open question for future study. Additional field studies and genetic analysis of this subgroup are sure to help clarify many of these questions and help to understand the ecological and evolutionary dynamics of populations with relevance to human health and otherwise.

References:

770 Aminetzach YT, Macpherson JM, Petrov DA (2005) Pesticide resistance via
771 transposition-mediated adaptive gene truncation in Drosophila. *Science*
772 *(New York, N.Y.)*, **309**, 764–767.
773 Caputo B, Santolamazza F, Vicente JL *et al.* (2011) The "far-west" of Anopheles
774 gambiae molecular forms. *PloS one*, **6**, e16415.
775 Charlesworth B (1998) Measures of divergence between populations and the effect
776 of forces that reduce variability. *Molecular Biology and Evolution*, **15**, 538–
777 543.
778 Charlesworth D, Charlesworth B (1987) Inbreeding Depression and its Evolutionary
779 Consequences. *Annual Review of Ecology and Systematics*, **18**, 237–268.
780 Coluzzi M, Sabatini A, Petrarca V, Di Deco MA (1979) Chromosomal differentiation
781 and adaptation to human environments in the Anopheles gambiae complex.
782 *Transactions of the Royal Society of Tropical Medicine and Hygiene*, **73**, 483–
783 497.
784 Coluzzi M, Sabatini A, della Torre A, Di Deco MA, Petrarca V (2002) A polytene
785 chromosome analysis of the Anopheles gambiae species complex. *Science*
786 *(New York, N.Y.)*, **298**, 1415–1418.
787 Corbett-Detig RB, Hartl DL (2012) Population genomics of inversion polymorphisms
788 in Drosophila melanogaster. *PLoS genetics*, **8**, e1003056.
789 Costantini C, Ayala D, Guelbeogo WM *et al.* (2009) Living at the edge: biogeographic
790 patterns of habitat segregation conform to speciation by niche expansion in
791 Anopheles gambiae. *BMC Ecology*, **9**, 16.
792 Crawford JE, Riehle MM, Guelbeogo WM *et al.* (2015) Reticulate Speciation and
793 Barriers to Introgression in the Anopheles gambiae Species Complex.
794 *Genome Biology and Evolution*, **7**, 3116–3131.
795 Cruickshank TE, Hahn MW (2014) Reanalysis suggests that genomic islands of
796 speciation are due to reduced diversity, not reduced gene flow. *Molecular*
797 *Ecology*, **23**, 3133–3157.
798 Dao A, Yaro AS, Diallo M *et al.* (2014) Signatures of aestivation and migration in
799 Sahelian malaria mosquito populations. *Nature*, **516**, 387–390.

DePristo MA, Banks E, Poplin R *et al.* (2011) A framework for variation discovery and genotyping using next-generation DNA sequencing data. *Nature genetics*, **43**, 491–498.

Fanello C, Santolamazza F, della Torre A (2002) Simultaneous identification of species and molecular forms of the Anopheles gambiae complex by PCR-RFLP. *Medical and veterinary entomology*, **16**, 461–464.

Feder JL, Xie X, Rull J *et al.* (2005) Mayr, Dobzhansky, and Bush and the complexities of sympatric speciation in Rhagoletis. *Proceedings of the National Academy of Sciences of the United States of America*, **102 Suppl 1**, 6573–6580.

Fontaine MC, Pease JB, Steele A *et al.* (2015) Mosquito genomics. Extensive introgression in a malaria vector species complex revealed by phylogenomics. *Science (New York, N.Y.)*, **347**, 1258524.

Gazal S, Sahbatou M, Babron M-C, Génin E, Leutenegger A-L (2014) FSuite: exploiting inbreeding in dense SNP chip and exome data. *Bioinformatics (Oxford, England)*, **30**, 1940–1941.

Gnémé A, Guelbéogo WM, Riehle MM *et al.* (2013) Equivalent susceptibility of Anopheles gambiae M and S molecular forms and Anopheles arabiensis to Plasmodium falciparum infection in Burkina Faso. *Malaria Journal*, **12**, 204.

Griffin JT, Hollingsworth TD, Okell LC *et al.* (2010) Reducing Plasmodium falciparum Malaria Transmission in Africa: A Model-Based Evaluation of Intervention Strategies. *PLoS Med*, **7**, e1000324.

Gutenkunst RN, Hernandez RD, Williamson SH, Bustamante CD (2009) Inferring the Joint Demographic History of Multiple Populations from Multidimensional SNP Frequency Data. *PLoS Genet*, **5**, e1000695.

Hamilton WD, Axelrod R, Tanese R (1990) Sexual reproduction as an adaptation to resist parasites (a review). *Proceedings of the National Academy of Sciences of the United States of America*, **87**, 3566–3573.

Holt RA, Subramanian GM, Halpern A *et al.* (2002) The genome sequence of the malaria mosquito Anopheles gambiae. *Science (New York, N.Y.)*, **298**, 129–149.

Korneliussen T, Albrechtsen A, Nielsen R (2014) ANGSD: Analysis of Next Generation Sequencing Data. *BMC bioinformatics*, **15**, 356.

Krzywinski MI, Schein JE, Birol I *et al.* (2009) Circos: An information aesthetic for comparative genomics. *Genome Research*.

Lee Y, Marsden CD, Norris LC *et al.* (2013) Spatiotemporal dynamics of gene flow and hybrid fitness between the M and S forms of the malaria mosquito, Anopheles gambiae. *Proceedings of the National Academy of Sciences*, 201316851.

Leutenegger A-L, Labalme A, Genin E *et al.* (2006) Using genomic inbreeding coefficient estimates for homozygosity mapping of rare recessive traits: application to Taybi-Linder syndrome. *American Journal of Human Genetics*, **79**, 62–66.

Leutenegger A-L, Sahbatou M, Gazal S, Cann H, Génin E (2011) Consanguinity around the world: what do the genomic data of the HGDP-CEPH diversity panel tell us? *European journal of human genetics: EJHG*, **19**, 583–587.

Li H (2013) Aligning sequence reads, clone sequences and assembly contigs with BWA-MEM. *arXiv:1303.3997 [q-bio]*.

Li H, Handsaker B, Wysoker A *et al.* (2009) The Sequence Alignment/Map format and SAMtools. *Bioinformatics (Oxford, England)*, **25**, 2078–2079.

Luong LT, Heath BD, Polak M (2007) Host inbreeding increases susceptibility to ectoparasitism. *Journal of Evolutionary Biology*, **20**, 79–86.

Medley GF, Sinden RE, Fleck S *et al.* (1993) Heterogeneity in patterns of malarial oocyst infections in the mosquito vector. *Parasitology*, **106 (Pt 5)**, 441–449.

Mitri C, Markianos K, Guelbeogo WM *et al.* (2015) The kdr-bearing haplotype and susceptibility to Plasmodium falciparum in Anopheles gambiae: genetic correlation and functional testing. *Malaria Journal*, **14**, 391.

Molineaux L, Gramiccia G, Organization WH (1980) The Garki project : research on the epidemiology and control of malaria in the Sudan savanna of West Africa.

Murray CJ, Rosenfeld LC, Lim SS *et al.* (2012) Global malaria mortality between 1980 and 2010: a systematic analysis. *The Lancet*, **379**, 413–431.

860 Navarro A, Barton NH (2003) Chromosomal Speciation and Molecular Divergence--
861 Accelerated Evolution in Rearranged Chromosomes. *Science*, **300**, 321–324.
862 Ndiath MO, Brengues C, Konate L *et al.* (2008) Dynamics of transmission of
863 Plasmodium falciparum by Anopheles arabiensis and the molecular forms M
864 and S of Anopheles gambiae in Dielmo, Senegal. *Malaria journal*, **7**, 136.
865 Niare O, Markianos K, Volz J *et al.* (2002) *Genetic loci affecting resistance to human*
866 *malaria parasites in a West African mosquito vector population*.
867 Nielsen R, Korneliussen T, Albrechtsen A, Li Y, Wang J (2012) SNP calling, genotype
868 calling, and sample allele frequency estimation from New-Generation
869 Sequencing data. *PloS one*, **7**, e37558.
870 Noor MAF, Bennett SM (2009) Islands of speciation or mirages in the desert?
871 Examining the role of restricted recombination in maintaining species.
872 *Heredity*, **103**, 439–444.
873 Noor MA, Grams KL, Bertucci LA, Reiland J (2001) Chromosomal inversions and the
874 reproductive isolation of species. *Proceedings of the National Academy of*
875 *Sciences of the United States of America*, **98**, 12084–12088.
876 Oliveira E, Salgueiro P, Palsson K *et al.* (2008) High levels of hybridization between
877 molecular forms of Anopheles gambiae from Guinea Bissau. *Journal of*
878 *medical entomology*, **45**, 1057–1063.
879 Riehle MM, Guelbeogo WM, Gneme A *et al.* (2011) A cryptic subgroup of Anopheles
880 gambiae is highly susceptible to human malaria parasites. *Science (New York,*
881 *N.Y.)*, **331**, 596–598.
882 Rieseberg LH (2001) Chromosomal rearrangements and speciation. *Trends in*
883 *ecology & evolution*, **16**, 351–358.
884 Santolamazza F, Mancini E, Simard F *et al.* (2008) Insertion polymorphisms of
885 SINE200 retrotransposons within speciation islands of Anopheles gambiae
886 molecular forms. *Malaria journal*, **7**, 163.
887 Schlenke TA, Begun DJ (2004) Strong selective sweep associated with a transposon
888 insertion in Drosophila simulans. *Proceedings of the National Academy of*
889 *Sciences of the United States of America*, **101**, 1626–1631.

Sharakhova MV, George P, Brusentsova IV *et al.* (2010) Genome mapping and characterization of the Anopheles gambiae heterochromatin. *BMC genomics*, **11**, 459.

della Torre A, Fanello C, Akogbeto M *et al.* (2001) Molecular evidence of incipient speciation within Anopheles gambiae s.s. in West Africa. *Insect Molecular Biology*, **10**, 9–18.

Vieira FG, Fumagalli M, Albrechtsen A, Nielsen R (2013) Estimating inbreeding coefficients from NGS data: Impact on genotype calling and allele frequency estimation. *Genome research*, **23**, 1852–1861.

White BJ, Santolamazza F, Kamau L *et al.* (2007) Molecular karyotyping of the 2La inversion in Anopheles gambiae. *The American journal of tropical medicine and hygiene*, **76**, 334–339.

WHO (2013) World Malaria Report.

Zheng L, Benedict MQ, Cornel AJ, Collins FH, Kafatos FC (1996) An integrated genetic map of the African human malaria vector mosquito, Anopheles gambiae. *Genetics*, **143**, 941–952.

Acknowledgements

We thank Matteo Fumagalli, Filipe Vieira, and Tyler Linderoth for assistance with next generation sequence data analyses and ANGSD. We thank members of the Nielsen group for helpful discussions on various aspects of this work and comments on an earlier version of this manuscript. We also thank multiple anonymous reviewers. We are thankful for the use of the Extreme Science and Engineering Discovery Environment (XSEDE), which is supported by National Science Foundation grant number OCI-1053575. This work was also supported by a National Institutes of Health Ruth L. Kirschstein National Research Service Award and a Cornell Center for Comparative and Population Genomics Graduate Fellowship to JEC.

Data Accessibility

Sequence data generated for this study can be accessed through the Short Read Archive at NCBI under BioProject ID PRJNA273873.

Author Contributions

JEC wrote software and analyzed data; KDV, MMR, WMG, AG, NS contributed new reagents and analytical tools; JEC, BPL, KDV, MMR, and RN designed research. JEC wrote the manuscript with contributions from the rest of the authors.

Tables

Table 1: Optimized parameter values and confidence intervals from the maximum-likelihood demographic model for GOUNDRY and *A. coluzzii*. See Figure 2 for parameter descriptions.

Parameter	**Optimized Value**	**95% Confidence Interval**	
		Lower	Upper
θ ($4N_A\mu L$)[a]	180,914		
N_A[b]	126,252	88,916	150,976
Split Times			
t_1	259,220	114,087	396,171
t_2	754,204	741,946	766,215
t_3	99,235	93,113	105,754
t_{TOT}	1,112,660	967,181	1,250,106
Population sizes			
N_{Ac1}/N_A	0.01	0.01	0.01
N_{Ac2}/N_A	5.74	4.58	7.65
N_{Ac3}/N_A	12.34	9.54	16.61
N_{G1}/N_A	0.01	0.00*	0.08
N_{G2}/N_A	0.19	0.11	0.32
N_{G3}/N_A	0.78	0.62	1.05
Migration rates (4Nm)[c]			
G1 into *Ac*1	0.010	0.0047	0.02

G2 into *Ac*2	1.29	1.25	1.33
G3 into *Ac*3	0.37	0.08	0.74
*Ac*1 into G1	0.080	0.00*	0.64
*Ac*2 into G2	1.17×10^{-4}	0.00*	0.0015
*Ac*3 into G3	1.50	1.44	1.55

a – Instead of estimating a confidence interval for θ which itself is not model parameter, we solved for N_A and calculated a confidence for this parameter. In the implementation of *dadi*, N_A is used to scale all other parameters in the model.

b – Ancestral population size was calculated from the estimate of θ by dividing this value by 4 times the number of sites times the mutation rate (see Methods above).

c – Values of $4Nm$ were calculated by multiplying the migration rate reported by *dadi* ($2N_Am$) by 2 times the ratio of the effective size of the recipient population (e.g. N_{G1}) over N_A.

* indicates cases where the lower bound of the 95% CI was negative. This is not meaningful, so we set these values to 0.

Table 2: Association between inbreeding coefficients and *Plasmodium* infection prevalence.

Cutoff[b]	**Inbreeding Level**[a]				X^2 **value**	***P* value**[c]
	Low		**High**			
	Infected	Not infected	Infected	Not infected		
0.0260	77	60	93	44	3.4870	0.0205
0.0292	81	60	89	44	2.2200	0.0546

a – Inbreeding coefficient class

b – Cutoff used to assign individuals to low or high inbreeding class. Individuals were assigned to low class if their *F* value was less than or equal to this cutoff. See text for explanation choice of cutoff values.

c – *P* values were calculated by comparing the empirical X^2 value to X^2 values obtained from 10^4 permuted datasets in a one-tailed test (See Methods).

Figure Legends

Figure 1: Average genetic relationships among species and subgroups in *Anopheles gambiae* species complex. Unrooted neighbor-joining tree calculated with the *ape* package in R and drawn with Geneious software. Branches indicate genetic distance (D_{xy}) calculated using intergenic sites (see Methods) with scale bar for reference. Bootstrap support percentages are indicated on all internal nodes. Branch lengths and 95%CIs indicated for branches leading to *A. merus* and *A. arabiensis*.

Figure 2: 2D-Site frequency spectrum and demographic model fitting of GOUNDRY and *A. coluzzii*. A) Three-epoch demographic model. One and two-epoch models have parameters from only first (Epoch 1) or first and second epochs, respectively. *N* parameters indicate effective population sizes. The duration of each epoch is specified by *t* parameters. Migration parameters ($2Nm$) are included as functions of the ratio of epoch-specific effective sizes relative to the ancestral effective size. We included separate migration parameters for *A. coluzzii* into GOUNDRY migration ($2N_A m_{GC}$) and GOUNDRY into *A. coluzzii* ($2N_A m_{CG}$). **B)** Autosomal, unfolded two-dimensional site-frequency spectrum (2D-sfs) for GOUNDRY and *A. coluzzii* for empirical data. **C)** 2D-sfs (top row) for maximum-likelihood models under four demographic models. Residuals are calculated for each model comparison (bottom row) as the normalized difference between the model and the data (model – data), such that red colors indicate an excess number of SNPs predicted by the model. See Table 1 for parameter values of the best-fit models under each demographic scenarios.

Figure 3: Chromosomal distributions of nucleotide diversity (π) at inter-genic sites (LOESS-smoothed with span of 1% using 10 kb non-overlapping windows). Low complexity and heterochromatic regions were excluded. The strong reduction of diversity on the X chromosome in GOUNDRY (Mb 8.47 – 10.1) corresponds to putative chromosomal inversion X*h*.

Figure 4: Modeling expected values of Relative Node Depth (D_{GAc}/D_{GAg}). A) Expected values of RND when ancestral population sizes are assumed to be equal. Colors indicate the expectations under different relative split times. **B)** Expected values with t_{GAg} split time fixed to 1.1 (top) times the split time between GOUNDRY and *A. coluzzii* (t_{GAc}) or 1.5 times (bottom). Colors indicated relative effective sizes of ancestral populations. Values are plotted as a function of the GOUNDRY-*A.coluzzii* effective size (x-axis). Grey bar indicates 95% confidence interval demographic estimate for GOUNDRY-*A. coluzzii* ancestral size (see Methods).

Figure 5: Relative genetic divergence (D_a) between GOUNDRY and *A. coluzzii*. D_a plotted as a function of nucleotide diversity (*A. coluzzii*) using only intergenic sites in non-overlapping 10 kb windows. Low complexity and heterochromatic regions were excluded. X-Free: freely recombining regions on X chromosome. X-Inv: region inside putative X*h* chromosomal inversion. Non-parametric Mann-Whitney test indicates that relative divergence (D_a) is significantly higher inside X*h* ($P < 2.2\times10^{-16}$), consistent with this region acting as barrier to gene flow.

Figure 6: GOUNDRY genomes harbor long tracts of Identity-By-Descent. A) Comparison between rates of IBD in one representative *A. coluzzii* diploid (black; 'Ac' in figure) and one representative GOUNDRY diploid on the 3L chromosomal arm (Orange; 'G' in figure) plotted in physical distance. Top panel shows Loess-smoothed estimate of heterozygosity in 1 kb windows and bottom panel shows IBD tracts called with FSuite (Methods). *A. coluzzi* individuals do not harbor long IBD tracts, and heterozygosity within GOUNDRY individuals is comparable to heterozygosity in *A. coluzzii* except in long regions of homozygosity. **B)** Genetic position and size of IBD regions (orange bands) called with FSuite. **C)** Genetic position and size of IBD tracts called with FSuite for six additional GOUNDRY individuals. Small breaks in long IBD tracts reflect rare genotype errors causing erroneous break in IBD tract.

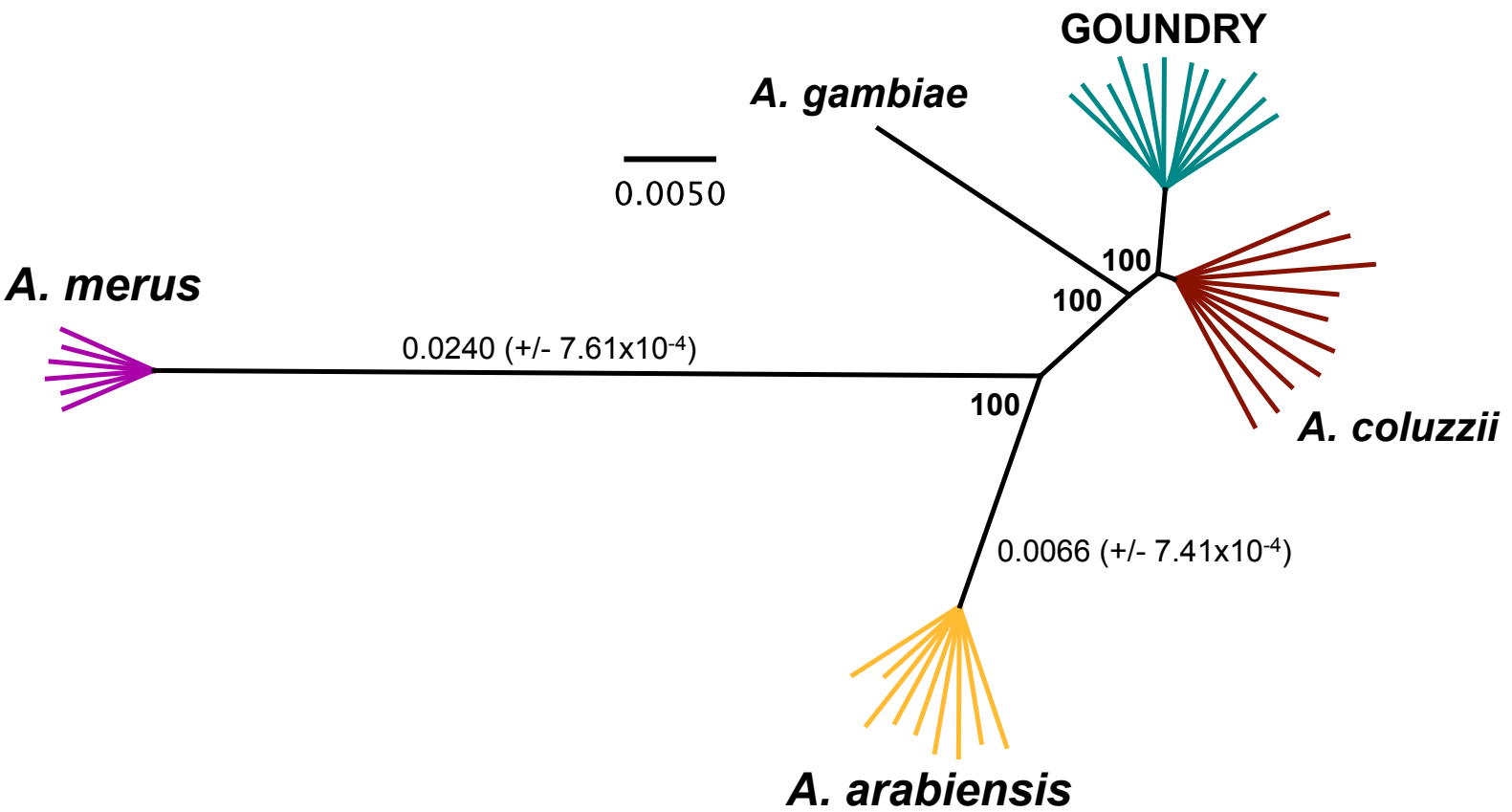
GOUNDRY
A. gambiae
0.0050
A. merus
100
100
0.0240 (+/- 7.61x10-4)
100
A. coluzzii
0.0066 (+/- 7.41x10-4)
A. arabiensis

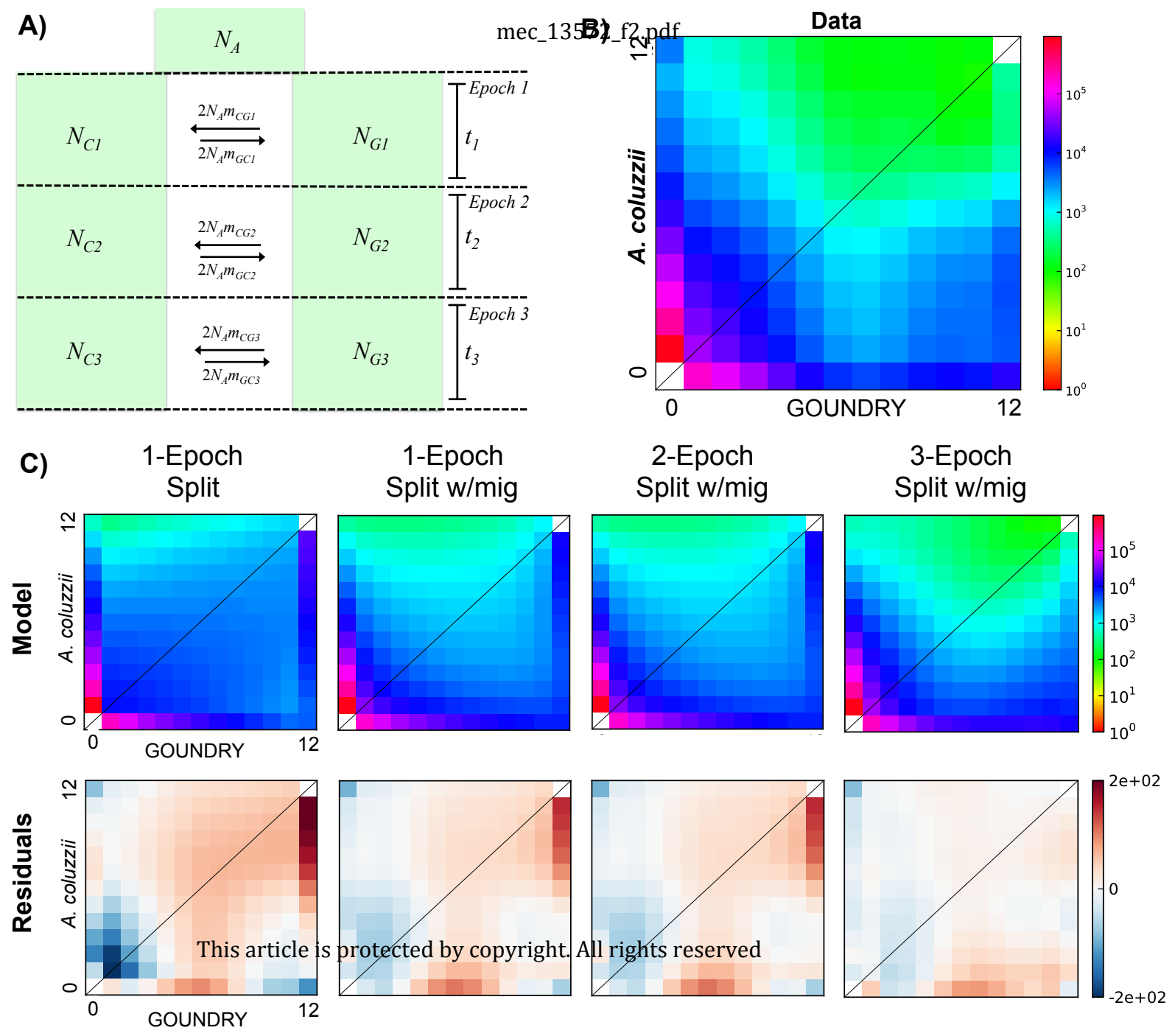

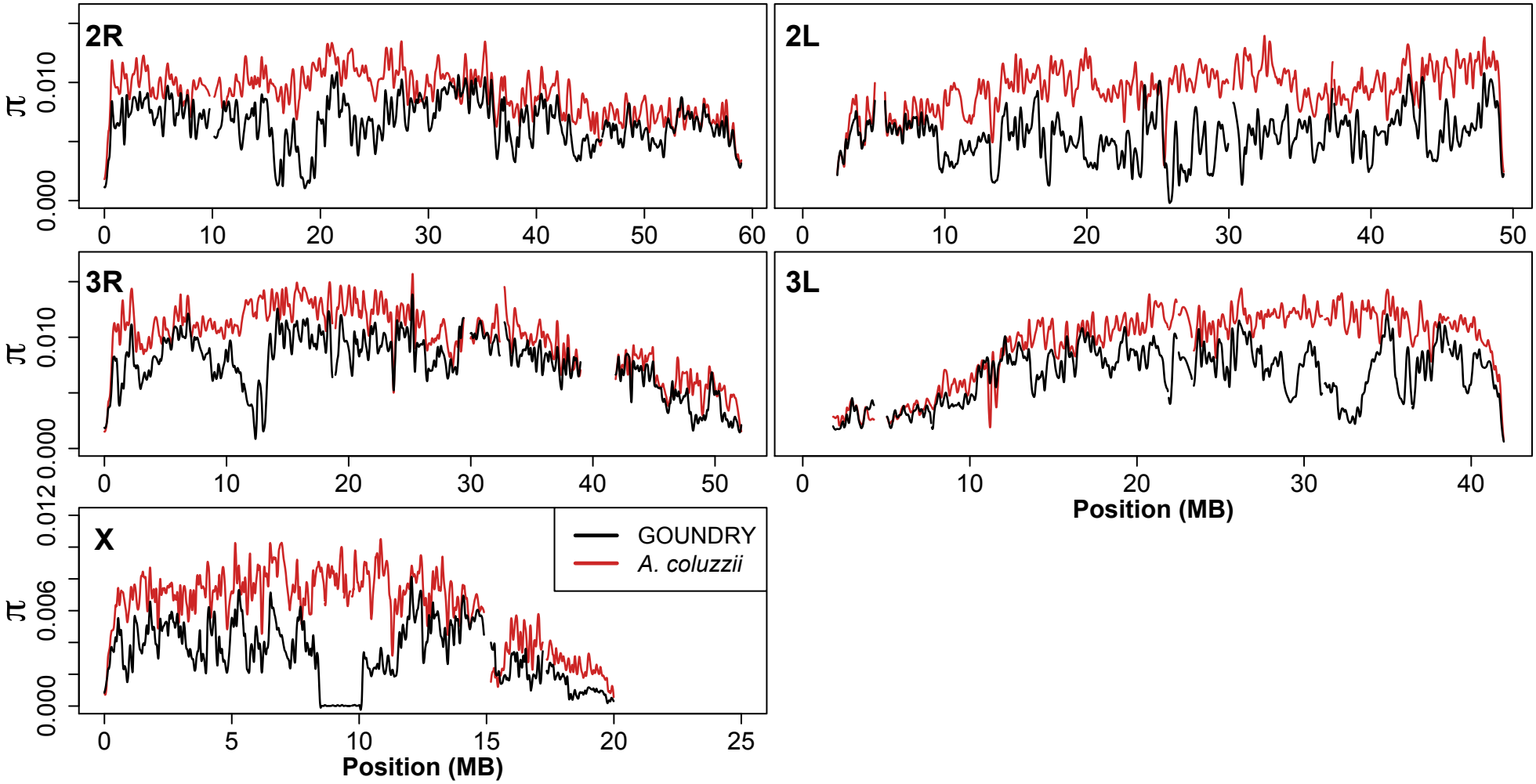
2R
2L
3R
3L
X
π
0.000
0.010
0.012
0.006
0
10
20
30
40
50
60
5
15
25
Position (MB)
GOUNDRY
A. coluzzii

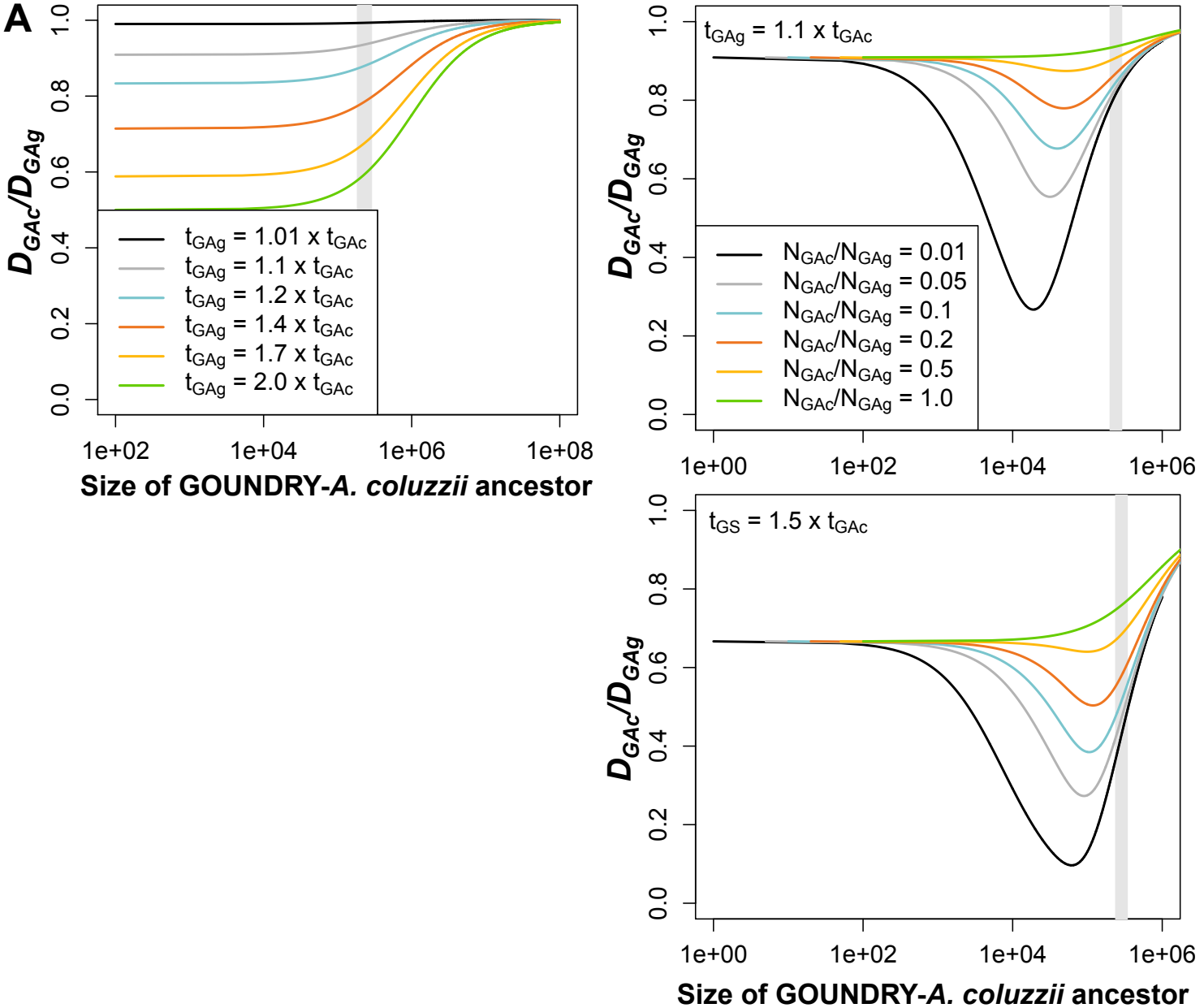
A
D_{GAc}/D_{GAg}
0.0
0.2
0.4
0.6
0.8
1.0
t_{GAg} = 1.01 x t_{GAc}
t_{GAg} = 1.1 x t_{GAc}
t_{GAg} = 1.2 x t_{GAc}
t_{GAg} = 1.4 x t_{GAc}
t_{GAg} = 1.7 x t_{GAc}
t_{GAg} = 2.0 x t_{GAc}
1e+02
1e+04
1e+06
1e+08
Size of GOUNDRY-*A. coluzzii* ancestor
t_{GAg} = 1.1 x t_{GAc}
N_{GAc}/N_{GAg} = 0.01
N_{GAc}/N_{GAg} = 0.05
N_{GAc}/N_{GAg} = 0.1
N_{GAc}/N_{GAg} = 0.2
N_{GAc}/N_{GAg} = 0.5
N_{GAc}/N_{GAg} = 1.0
1e+00
1e+02
1e+04
1e+06
t_{GS} = 1.5 x t_{GAc}
Size of GOUNDRY-*A. coluzzii* ancestor

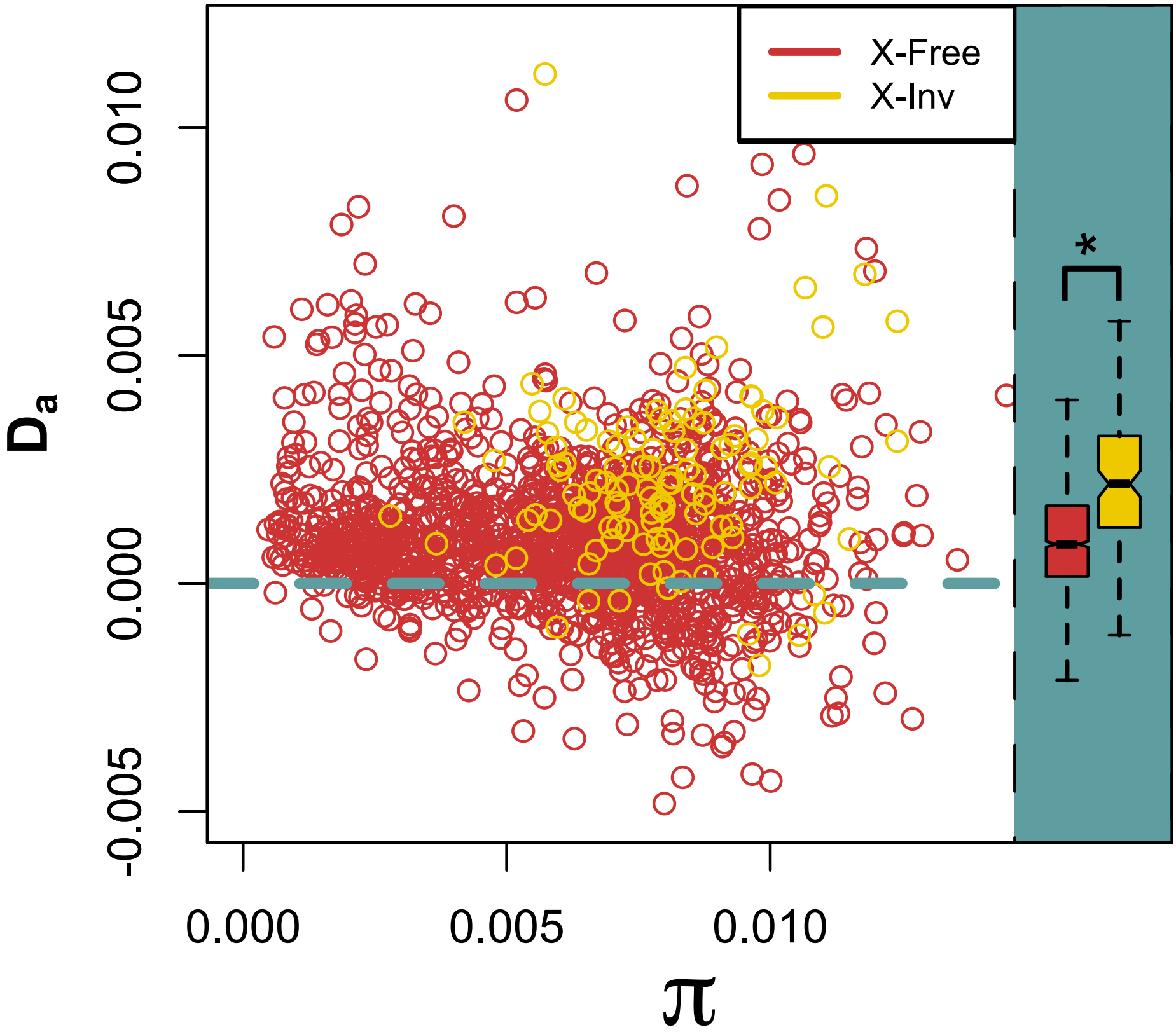
X-Free
X-Inv
*
D_a
0.010
0.005
0.000
-0.005
0.000
0.005
0.010
π

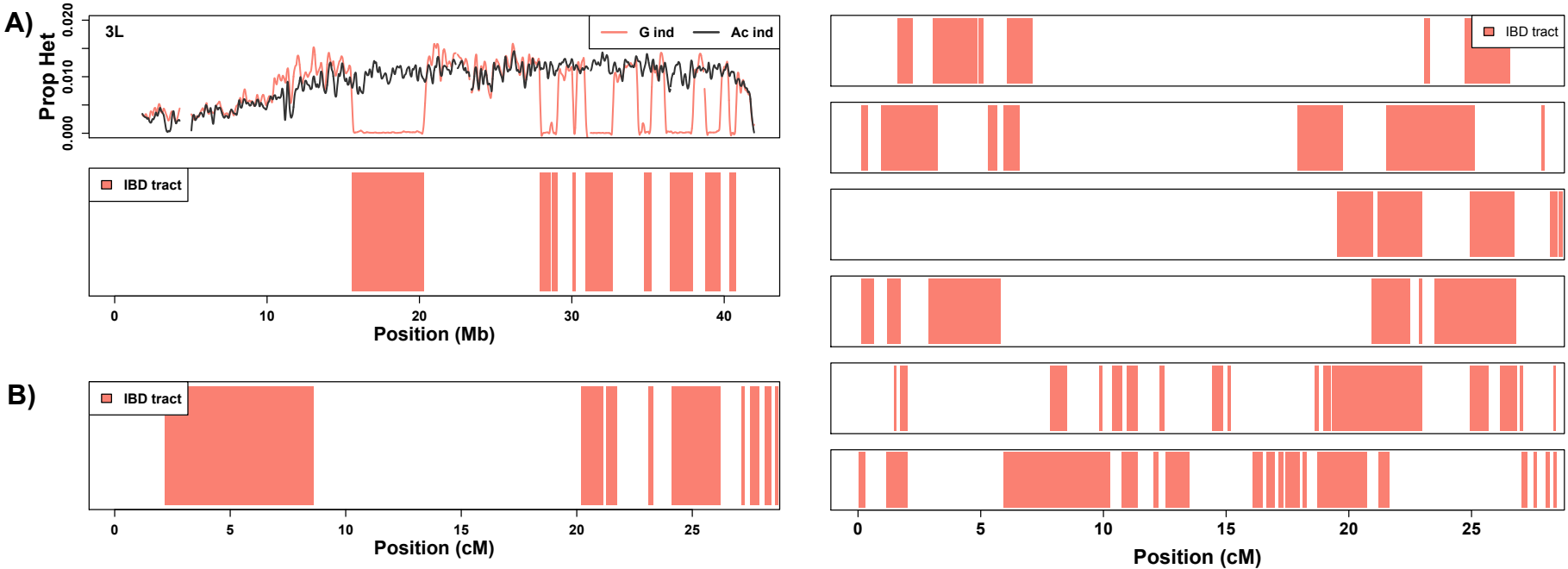
A)
3L
Prop Het
0.000
0.010
0.020
G ind
Ac ind
IBD tract
0
10
20
30
40
Position (Mb)
B)
IBD tract
0
5
10
15
20
25
Position (cM)
IBD tract
0
5
10
15
20
25
Position (cM)